Geochemical Journal, Vol. 39, pp. 469 to 480, 2005

Gas compositions and helium isotopic ratios of fluid samples around Kueishantao, NE offshore Taiwan and its tectonic implications

TSANYAO FRANK YANG,[1]* TEFANG FAITH LAN,[1] HSIAO-FEN LEE,[1] CHING-CHOU FU,[1] PEI-CHUAN CHUANG,[1] CHING-HUA LO,[1] CHENG-HONG CHEN,[1,2] CHEN-TUNG ARTHUR CHEN[3] and CHAO-SHING LEE[4]

[1]Department of Geosciences, National Taiwan University, P.O. Box 13-318, Taipei 106, Taiwan
[2]National Applied Research Laboratories, Taipei 106, Taiwan
[3]Institute of Marine Geology and Chemistry, National Sun Yat-Sen University, Kaohsiung 804, Taiwan
[4]Institute of Applied Geophysics, National Taiwan Ocean University, Keelung 202, Taiwan

(*Received March 20, 2005; Accepted July 20, 2005*)

Kueishantao is a Holocene volcanic islet (<7,000 yrs) located at NE offshore Taiwan, and tectonically is part of western extension of the Okinawa Trough. Magmatic activities are considered very active around this area on the basis of the fact that on-land fumaroles and submarine hydrothermal systems are prevailing currently. Representative bubble gas samples from submarine hydrothermal vents were collected for gas composition and helium isotope analysis. The gases show similar compositions of low temperatre fumaroles in the world, i.e., with high CO_2 and H_2S but low SO_2 and HCl contents. They exhibit consistent high $^3He/^4He$ ratios (7.3–8.4 R_A, where R_A is the $^3He/^4He$ ratio of air), probably the highest $^3He/^4He$ values of gases ever reported in active hydrothermal areas of the western Pacific region. Meanwhile, seawater samples around Kueishantao and other fluid samples from I-Lan Plain, the land area closest to the Kueishantao and also the southernmost part of the Okinawa Trough, show a significant excess of ^3He compositions as well. This indicates that the mantle component plays an important role for their gas sources, and implies that the mantle fluids may have invaded into I-Lan Plain. The westward opening of the Okinawa Trough may have caused thinning of the continental crust and produced deep normal faults and hence, the primordial ^3He is able to degas from mantle source region without significant crust contamination.

Keywords: $^3He/^4He$ ratios, Okinawa Trough, Kueishantao, hot springs, Taiwan

INTRODUCTION

Kueishantao (KST) is a young volcanic island located at the conjunction of the extension of the major fault system of northeastern Taiwan and the southernmost part of the Okinawa Trough (SPOT). Tectonically, this trough extends from SW Kyushu to NE Taiwan (Figs. 1A and B) and has been considered as an intracontinental backarc basin of the Ryukyu arc-trench system owing to subduction of the Philippine Sea plate underneath the Eurasian plate (Lee *et al*., 1980; Letouzey and Kimura, 1986; Sibuet *et al*., 1998). Due to the southwest-propagating of western edge of subducting Philippine Sea plate, the collision between Luzon arc and Eurasian plate was moving westward and induced spreading of the Okinawa Trough and consequently, caused the mountain collapse in northern Taiwan (Teng, 1996). Wang *et al*. (1999, 2004) proposed that the post-collisional extension in northern Taiwan could have triggered the Plio-Pleistocene volcanism of the Tatun Volcano Group (TVG in Fig. 1C), and its volcanic activities are considered to be non-dormant by Song *et al*. (2000).

Another area in northern Taiwan that subjected to the continuous subsidence is the I-Lan (IL) Plain (Fig. 1C). GPS data demonstrated that the west-bounding extension rate of this plain is 126 mm/y (Liu, 1995). A major thrust fault, the Li-Shan (LS) Fault, divides the Central Range and IL Plain in NE Taiwan and runs through the KST to the Okinawa Trouth (Sibuet *et al*., 1998). Tsai *et al*. (1975) reported a subsurface vertical fault less than 20 km deep, which runs from the IL Plain to KST, extending further to the Okinawa Trough in a NE direction. Recently, more than 70 active submarine volcanoes have been identified in the SPOT area (Lee *et al*., 1998). Those volcanoes, including KST, are located ~100 km above the Wadati-Benioff zone (Kao *et al*., 1998). In addition to the differences of structural and sedimentary events (Hsu *et al*., 1996; Park *et al*., 1998) recorded in SPOT and middle-northern part of the Trough, Chung *et al*. (2000) suggested that the SPOT is not a simple backarc basin but instead an embryonic rift zone in which early arc volcanism occurs as a result of the Ryukyu subduction. The estimated lithospheric structure based on calculation of isostatic

*Corresponding author (e-mail: tyyang@ntu.edu.tw)

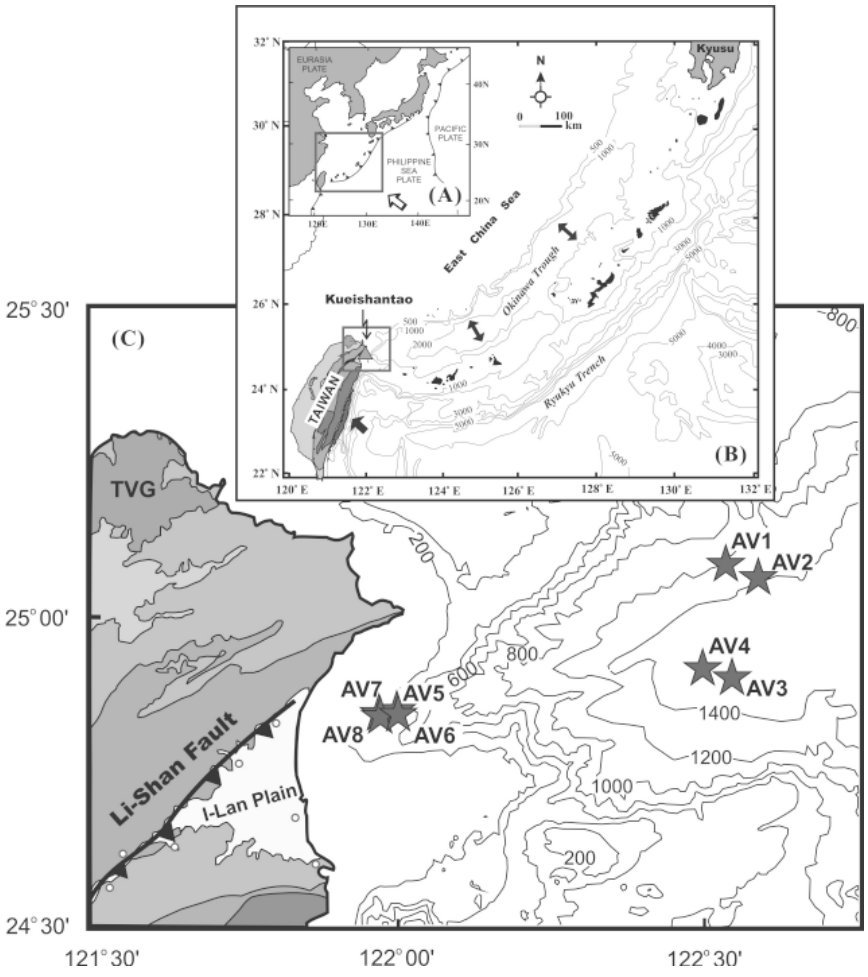

Fig. 1. Location of the studied area. (A) Simplified tectonic map around Taiwan. (B) Bathymetric map of Okinawa Trough. The triangular symbol indicates the location of Kueishantao islet offshore NE Taiwan. The marked rectangle is enlarged shown (C), which shows several identified submarine active venting sites, labeled as AV and marked as stars in southernmost part of the Okinawa Trough (Lee et al., 1998). At least four submarine hydrothermal venting sites (AV5–AV8) around Kueishantao islet have been found. Note that Kueishantao islet is smaller than the symbol size. The Tatun Volcano Group (TVG) in northern Taiwan is also hydrothermally active. Open circles are the on-land sampling sites in this study.

equilibrium in the region also supported the conclusion (Hsu, 2001).

KST is a volcanic island mainly composed of andesitic lava flows and pyroclastic deposits (Hsu, 1963; Chen, 1990). A siltstone xenolith sample has been dated to be ~7,000 yrs by thermoluminescence dating technique (Chen *et al*., 2001). Based on the Sr-Nd-O isotopic data, Chen *et al*. (1995) suggested that more than 30% of crustal sediments get involved in the KST magma genesis. Chung *et al*. (2000) compared the geochemical characteristics of KST lavas with those from Okinawa basin and Ryukyu arc and found that they are similar to those of pre-backarc rifting volcanic rocks from the central Ryukyu arc, and different from those of backarc basin lavas from the middle Okinawa Trough and the post-backarc rifting Ryukyu arc volcanics. Hence, they concluded that they are the products of arc magmatism instead of rifting products. Recently, Chu (2005) reported some high-Mg andesites in the KST and concluded that they can be result from partial melting of subducting sediments and subsequently melt-mantle interaction.

The helium isotopic ratios of terrestrial materials can be identified as deriving from four components. They are: (1) Air: its $^3He/^4He$ ratio is very homogeneous (1.39×10^{-6}) and is commonly used as global standard (1 R_A); (2) Crust: the helium isotopic ratios are much lower than air (0.1~0.01 R_A) because abundant ^4He gases are produced by the radiogenic elements in the crust; (3) Upper mantle: as represented by the mid-ocean ridge basalts (MORB), which show narrow range of helium isotopic

ratios ($8 \pm 1\ R_A$); (4) Lower mantle: hot spot basalts are believed to have trapped the primordial ^{3}He, and usually exhibit much higher ^{3}He/^{4}He ratios (>30 R_A) (e.g., Lupton, 1983; Farley and Neroda, 1998; Ozima and Podosek, 2002; Porcelli *et al*., 2002). Hence, the helium isotopic ratio is widely used as a useful tool to trace of relevant samples source domain (e.g., Yang *et al*., 2003b; Fu *et al*., 2005), especially in the magma activity (e.g., Sano *et al*., 1984; Sano and Wakita, 1985; Poreda *et al*., 1988; Hilton *et al*., 1995, 2002; Van Soest *et al*., 1998, 2002; Yang *et al*., 1999, 2003a; Notsu *et al*., 2001). Poreda and Craig (1989), who measured ^{3}He/^{4}He ratios of volcanic gases from Circum-Pacific active volcanic arcs, showed that the dominant source of helium was the mantle wedge rather than subducted oceanic crust or sediment, both of which are rich in radiogenic ^{4}He. Combined with other geochemical data, Hilton *et al*. (1995) and Van Soest *et al*. (1998, 2002) used the helium isotopic results to resolve the sediment subduction and crustal contamination for the genesis of an arc magma.

A cluster of over 30 vents, at a water depth of about 10–20 m offshore the northeastern Taiwan, emits hydrothermal fluids and volcanic gases (Chen *et al*., 2005a, b). Many hot and cold springs also occur in IL Plain, where is the land area closest to the KST and also is the southernmost part of SPOT. Those fluid and bubble samples are believed can provide important information for the magma sources of KST and regional tectonic evolution. Therefore, representative samples, including those from on-land IL Plain and, sea surface and also submarines around KST, have been collected for gas composition and helium isotopic measurements in this study. Their results will be presented and used for further discussion on the tectonic implications of the area.

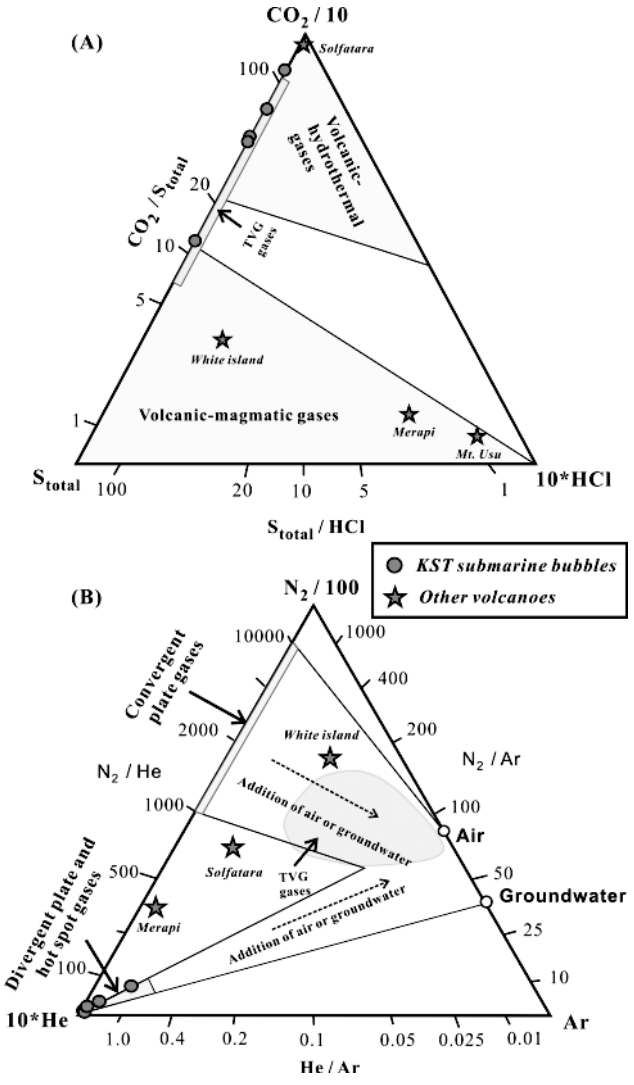

Fig. 2. Three component plots of the Kueishantao (KST) hot spring bubble gases. (A) In the CO_2-S_{total}-HCl plot, most KST samples fall in the range of volcanic hydrothermal gases and are similar with those TVG gases but show distinct deviations from the gases from other active volcanoes. (B) In the N_2-He-Ar plot, KST samples fall in the corner of the compositions of divergent plate and hot spot gases, which are significantly different from those from TVG and convergent plate gases. TVG gas data are from Lee et al. (2005); other volcanoes data are from Table 1. Gas boundaries are those described by Delmelle and Stix (2000).

Sampling and Measurements

Five bubble gas samples on sea surface around KST and three seawater samples from different water depths at the sites of AV1, AV2 and AV5 (Fig. 1C) were collected during the ORII cruised in June-July, 1999. Rest ten KST bubble gas samples were collected from the submarine venting sites by diving into the water depths of 10–20 m from 2000 to 2003. The sampling sites in IL Plain are shown in Fig. 1C. Bubbling samples are from Su-Au (SA) cold springs, Yuan-Shan (YS) bubbles, Ching-Suei (CS) hot springs, Fan-Fan (FF) hot springs, and Ren-Tzer (RZ) hot springs. Only water samples were collected from Jiao-Shi (JS) hot springs. Natural gases in Wu-Yuan (WY) were also collected. In contrast to most samples with CO_2 as major composition, WY gases are the only CH_4-dominant samples in this study.

The pre-evacuated low permeability glass bottles with two evacuated stopcocks at both ends were used for collecting the representative sea water and hot springs samples and, also the bubbling gas samples from hot and cold springs for the measurement of their gas compositions. The seawater samples were transferred to the glass bottles on board right after collected by Niskin bottles at different depths from 40 m to 1200 m during the OR II cruise in June, 1999. Bubbling samples were collected by the

Table 1. Dry gas compositions of bubbles from Kueishantao submarine hot springs and fumarolic gases from other volcanoes

Sample No.	Temp. (°C)	CO_2	H_2S	SO_2	HCl	He	H_2	Ar	O_2	N_2	CH_4	CO	Data source*	Note
Kueishantao (KST)														
001125-GSD-1	110	538	34.2	0.052	n.d.	0.024	25.5	3.50	56.0	338	5.0	n.d.	(1)	AC
001125-GSD-2	43	258	2.3	0.008	n.d.	0.040	6.90	6.10	108	618	1.6	n.d.	(1)	AC
030622-GSD-AVJ	55	978	20.4	0.271	0.028	0.028	0.114	0.009	0.195	0.871	b.d.l.	0.0004	(2)	
030622-GSD-VA	48	976	21.0	0.226	0.049	0.025	0.0007	0.025	0.032	2.231	0.335	0.0008	(2)	
030814-GSD-VA	56	992	8.46	0.073	0.023	0.015	0.021	0.001	0.011	0.108	0.035	<0.0001	(2)	
030814-GSD-VAK	107	987	12.6	0.009	0.023	0.007	0.003	0.0004	0.007	0.043	0.007	<0.0001	(2)	
030815-GSD-VAL	78	916	84.0	0.051	0.030	0.005	0.002	0.0002	0.002	0.024	0.030	<0.0001	(2)	
Tatun Volcano Group, N. Taiwan														
Da-you-keng fumarole	102	942	37.3	6.74	0.01	0.007	0.16	0.12	1.46	11.4	0.40	b.d.l.	(3)	
She-huang-ping hot springs bubbles	99.5	938	46.3	0.69	0.01	0.006	0.01	0.11	0.84	11.3	2.27	0.07	(3)	
Other volcanoes in the world														
Solfatara, Italy	97	992	2.99	b.d.l.	b.d.l.	0.010	0.78	0.004	n.d.	3.65	0.14	<0.001	(4)	
White Island, New Zealand	111	808	4.47	168	3.60	0.002	0.20	0.03	n.d.	9.8	8.9	n.d.	(5)	
Mt. Usu, Japan	690	575	29.3	52.2	68.0	n.d.	294	n.d.	n.d.	16.0	0.90	0.08	(5)	
Merapi, Gendol, Indonesia	803	489	13.0	95.4	53.8	0.004	44.3	4.29	1.59	319	n.d.	1.08	(6)	

**Data from (1) this study; (2) Chen et al. (2005b); (3) Lee et al. (2005); (4) Chiodini et al. (2001); (5) Giggenbach and Matsuo (1991); (6) Giggenbach et al. (2001).*
Note: All gas compositions shown as the unit of mmoles (10^{-3} mole) per mole. AC = air contaminated; b.d.l. = below detection limit; n.d. = not determined.

method of water replacement using a funnel covering on the top of bubbling sites. Those submarine bubble samples around KST showed strong sulfur smells. The so-called Giggenbach method, alkaline solution in the pre-evacuated Giggenbach bottles, was used to collected those acidic gases and then for further gas analysis (Giggenbach, 1975; Lee *et al*., 2005).

All the gas samples were analyzed by a gas chromatography system, which is equipped with two thermal conductivity detectors and one flame ionic detector, for determining their gas compositions first. The acidic gas samples collected with Giggenbach bottles need to do solution analysis for dissolved gases, including CO_2, HCl, H_2S and SO_2. The detailed analysis procedure and errors discussion has been described by Lee *et al*. (2005).

The analyzed samples were then sent for further helium isotopes measurement. $^3He/^4He$ and $^4He/^{20}Ne$ ratios have been measured with the Micromass 5400 noble-gas mass spectrometer with dual collectors in the Department of Geosciences, National Taiwan University. The system includes a two-stage purification line and a cryogenic pump with charcoal trap. The gas sample first passes through the first-stage purification line, including U cold-trap with liquid nitrogen, Cu-CuO furnace at 400°C, Ti-sponge furnace at 700°C, and charcoal trap with liquid nitrogen to remove most active gases (including H_2O, CO_2, N_2, O_2, H_2, hydrocarbon and sulfur gases etc.) and heavy noble gases (Ar, Kr, and Xe). Then the sample is allowed to enter the second-stage purification line for further purification. It includes Ti-sponge furnace, charcoal trap with liquid nitrogen, and SEAS Ti-Zr getters. At this stage all the active gases should be totally removed then, the purified gas can be trapped into a cryogenic pump at 15°K. At last, helium and neon are released by step-wisely increasing temperature, at 34°K and 70°K, respectively, to sequentially admit into the mass spectrometry for isotope measurement. Air is routinely run as a standard for calibration. A 20 R_A pure helium gas standard (Matsuda *et al*., 2002) is also prepared and run as working standard to reduce the analytical errors. In general, the total errors on the ratios are less than 2% and 5% for $^3He/^4He$ and $^4He/^{20}Ne$, respectively. Details of the measurements have been given by Yang (2000).

Analytical Results

The compositions of KST submarine bubble gases are shown in Table 1. Gases from TVG and other volcanoes in the world are also listed for comparison. Except for samples 001125-GSD-1 and -2 having significant air contamination with high N_2, O_2, Ar, most KST samples exhibit similar composition with TVG gases, i.e., high CO_2 (90–99%) and H_2S (0.8–8.4%) but low SO_2 (<0.03%) and HCl (<50 ppm) contents. It indicates that they have simi-

Table 2. Helium isotopic compositions around Kueishantao, NE offshore of Taiwan

Sample[1]	$^3He/^4He$ ($\times10^{-6}$)	$\pm1\sigma$ (%)	$[R/R_A]^2$	$^4He/^{20}Ne$	$[R_c/R_A]^3$	[He] (ppm)	X_M^4	Note[5]
Bubble gas samples collected on sea surface								
990620-KST-1	10.29	0.59	7.40	6.03	7.76 ± 0.19	—	97.0	
990622-KST-1	11.18	0.26	8.04	13.2	8.22 ± 0.21	—	100	
990622-KST-2	10.62	0.22	7.64	16.4	7.77 ± 0.19	—	97.1	
990706-KST-1	5.60	0.30	4.03	0.62	7.26 ± 0.18	—	90.7	X
990706-KST-2	6.75	0.34	4.86	0.81	7.38 ± 0.18	—	92.2	X
Bubble gas samples collected at submarine venting sites								
000516-GSD-2	11.30	0.27	8.13	9.13	8.39 ± 0.25	46.8	100	
001125-GSD-1	10.17	0.37	7.31	5.78	7.68 ± 0.19	23.7	96.0	
010324-GSD-1	10.07	0.18	7.25	19.0	7.35 ± 0.18	34.0	91.8	
010324-GSD-2	10.45	0.32	7.52	21.1	7.62 ± 0.22	35.7	95.2	
030622-GSD-AVJ	10.38	0.57	7.47	28.3	7.54 ± 0.12	24.6	94.2	
030622-GSD-VA	10.38	0.33	7.47	28.4	7.54 ± 0.11	28.0	94.2	
030814-GSD-VA	10.20	0.70	7.34	40.8	7.39 ± 0.13	15.0	92.3	
030814-GSD-VAK	10.41	1.41	7.49	46.4	7.53 ± 0.16	6.66	94.1	
030815-GSD-VAL	10.43	1.16	7.51	27.2	7.58 ± 0.15	5.18	94.7	
030815-GSD-VAM	10.28	1.41	7.40	32.6	7.46 ± 0.15	5.10	93.2	
Sea water samples					ΔHe^6			
990621-ST1-200	1.40	3.70	1.01	0.26	0.72	—	—	
990621-ST2-40	1.30	7.80	0.93	0.23	–6.47	—	—	
990621-ST5-1200	3.20	3.78	2.30	0.23	130.2	—	—	

1. The affix of the sample name (990620-) is the sampling date (99/06/20).
2. R: $^3He/^4He$ ratio of measured samples; R_A: ratio of air ($=1.39\times10^{-6}$).
3. R_c: air corrected helium isotopic ratio, assuming all the Ne derived from the air (Poreda and Craig, 1989).
4. X_M: percent of mantle component based on the calculation of Eq. (2).
5. X: R_c may not be properly corrected due to the He/Ne ratio (<1) is close to the ratio of air (0.319).
6. $\Delta He = [(R - R_A)/R_A] \times 100$.

lar gas compositions to those of typical low temperature fumaroles in the world and, are also consistent with the measured temperatures (43–110°C) at the venting sites.

Measured $^3He/^4He$ ratios of KST bubble samples range from 5.60 to 11.38×10^{-6} and $^4He/^{20}Ne$ ratios range from 0.62 to 46.4 (Table 2). If we assume that all the ^{20}Ne concentration of the sample comes from the atmosphere, then we can correct its helium ratio for atmospheric helium contamination by Eq. (1) (Poreda and Craig, 1989).

$$(^3He/^4He)_{cor} = [(^3He/^4He)_m - (^3He/^4He)\times r]/(1-r) \quad (1)$$

$$r = (^4He/^{20}Ne)_{air}/(^4He/^{20}Ne)_m.$$

Where the subscript *cor* is the corrected value; *m* is the measured value; *air* is the value of air.

The measured $^3He/^4He$ ratios are calibrated against atmospheric standard gas and are expressed relative to R_A, where R_A is the air $^3He/^4He$ ratio of 1.39×10^{-6}. All the KST samples, including bubbles from both sea surface and submarine, exhibit consistent high helium isotopic ratios after air correction, i.e., 7.35–8.39 R_A. It should be noted that samples 990906-KST-1 and -2, may not be properly corrected due to serious air contamination indicating by the very low $^4He/^{20}Ne$ ratios which close to the ratio of air (0.319) (Table 2). The high $^3He/^4He$ ratios, up to 8.4 R_A, are the highest values obtained so far from Taiwan, and probably are also the highest $^3He/^4He$ values of gases ever reported in active hydrothermal areas of the western Pacific region.

Assuming the measured sample is the mixture of mantle and crust components with the $^3He/^4He$ ratios of 8.0 and 0.05 R_A, respectively, then we can calculate the percentage of each component following Eq. (2).

$$R_c = 8.0\times X_M + 0.05\times(1 - X_M). \quad (2)$$

Where the subscript *c* is the corrected $^3He/^4He$ ratio; X_M is the percentage of mantle component involved in this sample. Percentage of crust component will be $(1 - X_M)$. It is clear that mantle component, X_M = 91–100%, is the dominant source for KST gas samples (Table 2). Note that

Table 3. Helium isotopic compositions of fluid samples from I-Lan Plain, NE Taiwan

Sample No.	Sample type[1]	$^4He/^{20}Ne$	$^3He/^4He$	$[R/R_A]^2$	$[R_c/R_A]^3 \pm 1\sigma$	[He] (ppm)	X_M^4
Wu-Yuan natural gas							
50309-WY-1	G	4.55	1.93×10^{-6}	1.39	1.42 ± 0.03	7.14	17.2
50403-WY-2	G	5.59	1.94×10^{-6}	1.40	1.42 ± 0.02	6.34	17.2
Su-Au cold springs							
90728-SA-2-2	BG	3.59	1.61×10^{-6}	1.16	1.17 ± 0.03	27.7	14.1
20223-SA-2-1	BG	7.33	1.77×10^{-6}	1.27	1.29 ± 0.03	33.4	15.6
20710-SA-1-1	BG	4.32	1.60×10^{-6}	1.15	1.17 ± 0.03	64.7	14.1
30227-SA-1	BG	14.8	1.70×10^{-6}	1.22	1.23 ± 0.04	36.7	14.8
30314-SA-1	BG	11.5	1.80×10^{-6}	1.29	1.30 ± 0.04	38.0	15.7
30404-SA-1	BG	15.5	1.71×10^{-6}	1.23	1.23 ± 0.03	42.1	14.8
Jiao-Shi hot springs							
90408-JS-2	W	7.75	0.56×10^{-6}	0.41	0.39 ± 0.01	—	4.3
30221-JS-2	W	8.73	0.54×10^{-6}	0.39	0.37 ± 0.01	61.8	4.0
30404-JS-2	W	5.09	0.57×10^{-6}	0.41	0.37 ± 0.01	41.2	4.0
30418-JS-1	W	9.94	0.54×10^{-6}	0.39	0.37 ± 0.01	39.4	4.0
Yuan-Shan bubbles							
30213-YS-2	BG	0.69	0.93×10^{-6}	0.67	0.39 ± 0.01	11.4	4.3
30519-YS-2	BG	0.63	1.02×10^{-6}	0.73	0.45 ± 0.01	11.5	5.0
30811-YS-2	BG	0.68	0.94×10^{-6}	0.67	0.39 ± 0.01	11.3	4.3
31009-YS-2	BG	0.82	0.92×10^{-6}	0.66	0.44 ± 0.01	17.2	4.9
Ching-Suei hot springs							
20223-CS-2	BG	0.73	1.82×10^{-6}	1.31	1.55 ± 0.04	2.27	18.9
20710-CS-2	BG	0.64	1.54×10^{-6}	1.11	1.22 ± 0.31	1.50	14.7
Fan-Fan hot springs							
30206-FF-1	BG	2.65	0.31×10^{-6}	0.22	0.12 ± 0.00	8.17	0.88
Ren-Tzer hot springs							
00819-RZ-2-1	BG	4.34	0.22×10^{-6}	0.16	0.09 ± 0.01	6.34	0.5
00828-RZ-2-2	BG	3.74	0.27×10^{-6}	0.20	0.12 ± 0.03	1.86	0.9

1. G = nature gas; W = water; BG = bubbling gas.
2. R: $^3He/^4He$ ratio of measured samples; R_A: ratio of air (1.39×10^{-6}).
3. R_c: air corrected helium isotopic ratio, assuming all the Ne derived from the air (Poreda and Craig, 1989).
4. X_M: percent of mantle component based on the calculation of Eq. (2).

two samples, 990622-KST-1 and 000516-GSD-2, have corrected $^3He/^4He$ ratios larger than 8.0. We treat them being derived from 100% mantle component contribution.

The seawater sample, 990621-ST5-1200, shows significant excess ^3He with $^3He/^4He$ ratio of 2.30 R_A in the dissolved gas (Table 2). It implies that mantle fluids are degassing into the sea from the active submarine volcanoes, although rest two seawater samples do not show excess ^3He.

Samples from IL Plain, in contrast to KST samples, show a wide range of $^3He/^4He$ ratios from 0.22 to 1.94×10^{-6} (Table 3). The ratios are from 0.09 to 1.55 R_A after air correction. They can be divided into two major groups. First group, including WY, SA and CS samples, shows significant mantle input, X_M = 14–19%. Second group, FF and RZ samples, has only very small amount of mantle contribution, X_M < 1%. JS and YS samples are not belonging to above two groups. They do not show clear mantle contributions but also have the elevated $^3He/^4He$ ratios, i.e., falling in the range between above groups with X_M = 4–5%.

Discussion

Gas sources and potential magma reservoir in the region

Similar to TVG gases, KST gases have very low HCl content but high CO_2/S_{total} ratios. Therefore, most KST data fall into the range of volcanic-hydrothermal gas composition in the plot of CO_2-S_{total}-HCl (Fig. 2A). Nevertheless, KST samples show higher He/Ar and lower N_2/He ratios and, fall in the composition of divergent plate and hot spot gases of the N_2-He-Ar plot (Fig. 2B). It is different from the TVG gases, which fall in the range of convergent plate gases. It implies that the KST and TVG

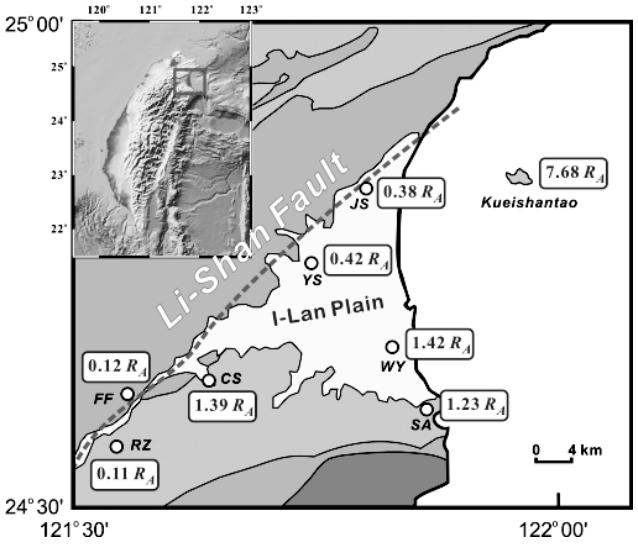

Fig. 3. Average helium isotopic compositions of fluid samples around Kueishantao and I-Lan Plain, NE Taiwan. The data are the air-corrected ratios from Tables 2 and 3. WY: Wu-Yuan natural gas; SA: Su-Au cold springs; JS: Jiao-Shi hot springs; YS: Yuan-Shan bubbles; CS: Ching-Suei hot springs; FF: Fan-Fan hot springs; RZ: Ren-Tzer hot springs.

gases may be derived from different tectonic environments. If those gases were derived from similar magmatic sources for lavas, then the result is consistent with the traditional tectonic model that the TVG samples were the product of Ryukyu arc subduction system; whereas, KST were the products of rifting of the Okinawa Trough (e.g., Teng, 1996).

Figure 3 shows the average air-corrected helium isotopic ratios of fluid samples in this study. The helium isotopic data of KST samples, including seawaters and bubbles, can be explained very well by binary end components mixing of air and MORB in the plot of $^3He/^4He$ vs. $^4He/^{20}Ne$ (Fig. 4). However, samples from IL Plain fall in the range between MORB, air and crust. They need ternary components mixing to account for their helium isotopic composition. For FF and RZ samples, nevertheless, they fall close to the mixing line between air and crust components. It indicates that only very few or even no MORB component is needed to account for their gas source.

The $^{20}Ne/^4He$ vs. $^3He/^4He$ ratio plot also shows the same result, and it is easier to estimate the relative proportions for each component, i.e., Air-Crust-Mantle, directly from diagram (Fig. 5). The estimation for the proportion of mantle component is similar to the result of the calculation from Eq. (2). The contribution of crust component for KST samples are very small and can be ignored. The KST submarine bubbles are dominant with mantle component (90–100%) and higher than those for TVG fumaroles (50–90%). For samples from IL Plain, in contrast, crust component clearly is their dominant source. YS and CS samples are mainly mixed by crust and air components, and with a little mantle component. Meanwhile, SA and WY gases, which do not have clear air contamination, exhibit higher mantle component than rest samples from IL Plain (i.e., CS, JS, YS, FF, and RZ).

The magma activity and existence of magma chamber in northern Taiwan have been concerned and debated by local geologists for long time. Recently, more data support that there may be existing magma chamber underneath TVG (Song *et al*., 2000; Yang, 2000; Lin *et al*., 2005). Chen and Shen (2005) reviewed some claimed historical eruptions in northern Taiwan and suggested that there were three records may be related to the magmatism of northern Taiwan volcanic zone and Quaternary Ryukyu volcanic front. Recently, Lin *et al*. (2004) analyzed the earthquake data to determine the three-dimensional V_p and V_s velocity structures in NE Taiwan and found a low V_s but high V_p/V_s sausage-like body, ~30 km in diameter, lies within the Eurasian mantle wedge, on the top of the most western part of Ryukyu slab. A low V_s but high V_p/V_s channel rises obliquely from the sausage-like body at a depth of 40 km in direction of KST. They further proposed that the H_2O-rich component and/or melt, i.e., magma, thus can rise up from the sausage-like body toward the surface via veins and/or narrow conduits. Their observation can support the high helium isotopic data around KST and suggest that there is a magma source underneath KST.

Invading of mantle fluids into the I-Lan Plain

Based on the continuous GPS data, Liu (1995) concluded that the IL Plain is propagating westward in the speed of 126 mm/y. He further estimated that the eastern part of IL Plain is subsiding in the rate of 20 mm/y due to the westward extension of the Okinawa Trough. Many normal faults have been recognized in SPOT and may be related to the NE extension of the on-land major fault, LS Fault, in IL Plain (Sibuet *et al*., 1998). It is clear that mantle component is necessary for most samples from IL Plain based on their elevated helium isotopic compositions (Fig. 3). If the mantle fluids have invaded into the IL Plain as suggested by present elevated helium isotopic data, the LS Fault may provide the major pathway for the mantle fluids migrating toward the shallower surface.

JS hot springs and YS bubbles are located along the LS Fault and closer to KST than other sampling sites in IL Plain. It was expected for them to exhibit highest helium isotopic ratios if the mantle fluids invade mainly through the LS Fault zone. However, the higher $^3He/^4He$ ratios are distributed in the southern part of IL Plain, i.e., WY, SA and CS, rather than in JS and YS. It indicates that the LS Fault is not the major pathway for the migra-

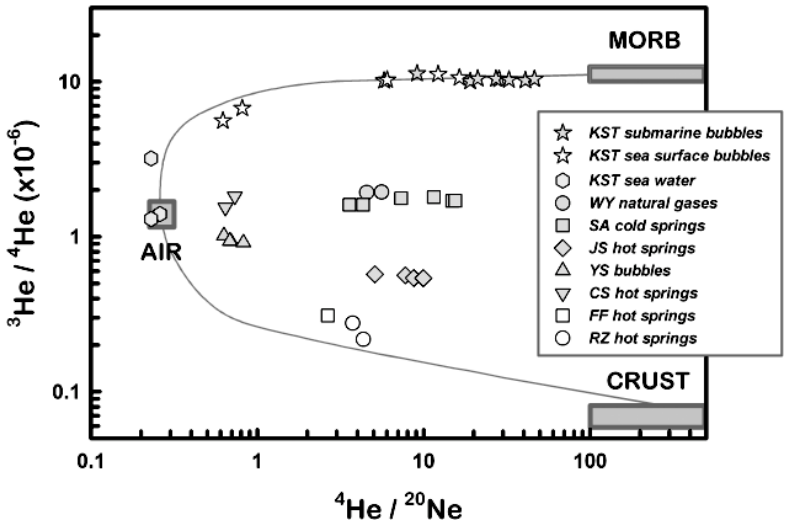

Fig. 4. $^3He/^4He$ *vs.* $^4He/^{20}Ne$ *plot for the fluid samples in this study. Acronyms are same as those in Fig. 3. All the KST samples, including bubbles and sea waters, exhibit higher* $^3He/^4He$ *ratios and fall in the mixing trend between Air component and MORB source component. Nevertheless, samples far away from KST, including FF and RZ hot springs, show much lower ratios with significant crustal signature. Note that samples from I-Lan Plain cannot be well explained by simple binary mixing of any two components.*

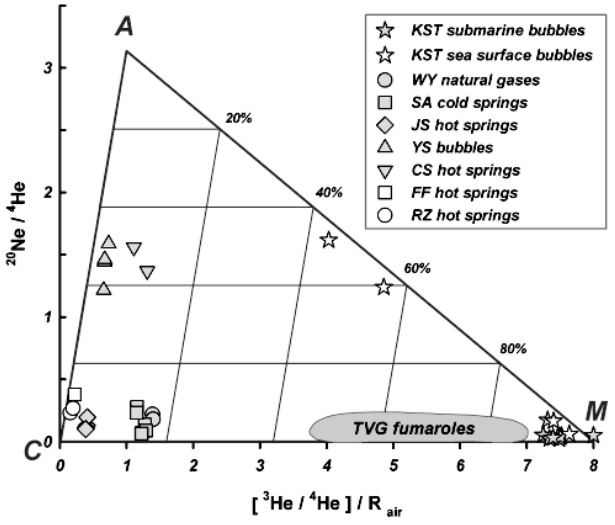

Fig. 5. The A-C-M three-component plot for fluid samples in this study. A: air; C: crust; M: MORB components. KST samples fall at the corner of MORB end component, indicating more than 90% of MORB source is necessary to account for their helium isotopic compositions. In addition to Air component, samples from I-Lan Plain (i.e., WY, SA, CS, and JS) also show elevated $^3He/^4He$ *ratios and need both Crust and MORB components to explain their geochemical characteristics. Fumaroles from TVG, typical of arc volcanic affinity, are also plotted for comparison (data from Yang et al., 1999; Yang, 2000).*

tion of mantle fluids. Therefore, we can further suggest that there would be a blind fault or magma intrusion in southern IL Plain to offer either the invading path or primordial ^3He source. Since the IL Plain is subsiding and the crust is thinning, alternatively, although the estimated crust in SPOT is ~25-30 km (Hsu, 2001), it could be able to generate some deep normal faults, as reported by Tsai *et al.* (1975), due to the extension of Okinawa Trough in the region. Therefore, the primordial ^3He is able to degas from mantle source region via the fault fractures.

Crust contamination vs. source contamination for KST magma

Chen *et al.* (1995) presented the very low Nd isotopic values (ε_{Nd} = –1.9 to –5.2), and very high Sr ratios ($^{87}Sr/^{86}Sr > 0.705$) and high $\delta^{18}O$ (between 7 and 8‰) with strong continental signature on KST lavas. They further explained the data resulting from a MORB-like magma assimilation with about 30% local continental crust materials and/or the thick overlying sediments during the onset of the rifting stage of the Okinawa Trough. However, present KST data seem not support the model, if the magma source of KST is mainly derived from upper mantle with the helium ratio of 8.0 R_A. Alternatively, if the KST magma is derived from a plume source with the helium isotopic ratio of 11 R_A, and mixed with 30% of continental curst with the $^3He/^4He$ ratio of 0.05 R_A, then it is able to generate the present KST average helium isotopic ratios of 7.68 R_A. However, there no current plume or hot spot source with high $^3He/^4He$ ratios (i.e., >10 R_A) have

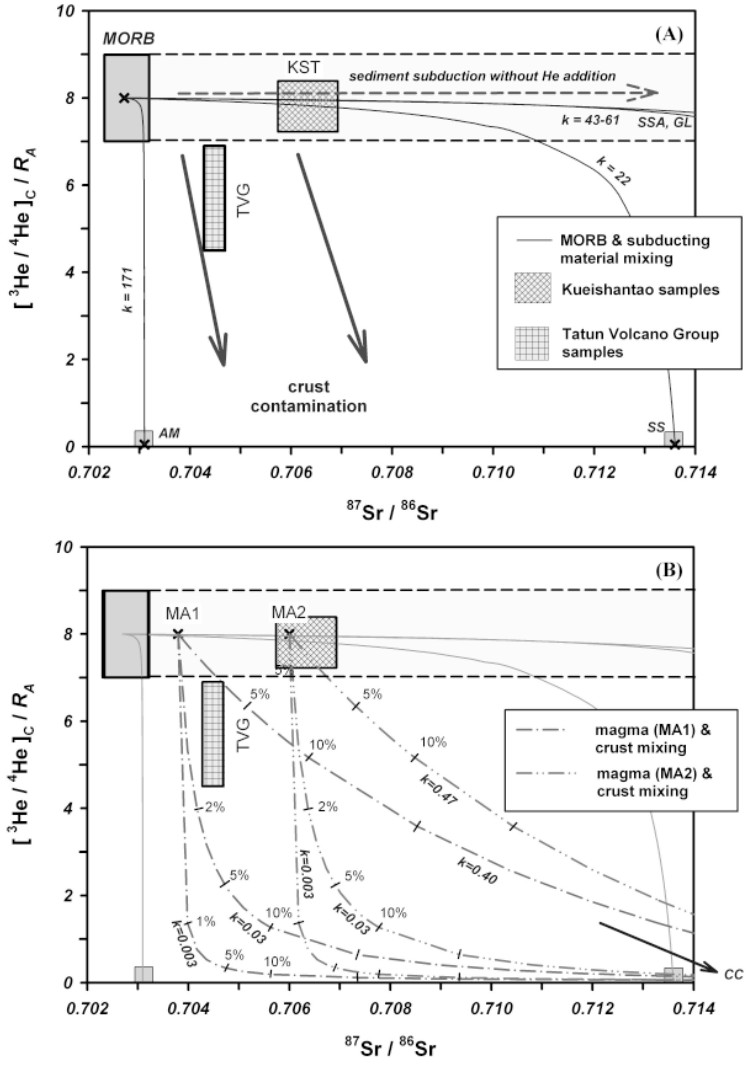

Fig. 6. Binary mixing curves of $^{3}He/^{4}He$ vs. $^{87}Sr/^{86}Sr$ end components. Assuming the compositions of the fumarolic gases from Kueishantao (KST) and Tatun Volcano Group (TVG) are similar with those of lavas. (A) MORB and subducted component mixing. The mixing curves represent an end-member scenario with the assumption of complete helium retention in the subducted components. The alternative scenario is presented by the dashed-line box extending from the MORB box towards higher $^{87}Sr/^{86}Sr$, labeled "sediment subduction without He addition". This represents the case where no helium survives the subduction process and subduction addition is reflected only the Sr isotopes. Thick arrows indicate the trend of crust contamination. It is clear that KST samples, unlike TVG samples, do not show significant crust contamination, but can be explained by the mixing of MORB source with subducted sediments (either case with or without additional helium). (B) Potential magmas mixing with different crustal components. KST samples fall in the range of potential magma 2 (MA2), which is generated at upper mantle level by mixing the MORB source with 30% Sr of subducted sediments before enter the crustal level, and then experienced minimum crustal contamination. In contrast, TVG samples can be explained by magma-crust mixing with the potential magma 1 (MA1) and various degrees of crust input (2–5%). Note that MA1 is the composition of MORB source adding 10% Sr of subducted sediments. Compositions of all the mixing end members are listed in Table 4. KST helium data are from this study; Sr data, from Chen et al. (1995) and Chu (2005); and TVG helium data, from Yang et al. (1999) and Yang (2000); Sr data, from Wang et al. (2004).

ever been reported in this region, although Macpherson *et al*. (1998) and Shaw *et al*. (2004) reported high $^{3}He/^{4}He$ ratios (up to 15 R_A) with a plume signature for lavas form the Manus backarc basin. Thus, it is unlikely to have such big amount of crust component input the magma source for the helium isotopic system.

People may argue that the present KST gas samples may be not derived from the same magma source for KST lavas. Before the last eruption occurred in KST 7,000 yrs ago (Chen *et al*., 2001), the thickness of the overlying

Table 4. End members for He-Sr mixing in the Fig. 6

End members[a]	[^{4}He] (ncm^{3}STP/g)	R_A	[Sr] (ppm)	^{87}Sr/^{86}Sr	Subduction mixing[b]	k[c]	Crustal mixing[d]	k[c]
MORB source (MS)	5000	8.00	9.0	0.7027	MS-AM	171	MA1-CC1	0.003
GLOSS (GL)	3000	0.05	327	0.7173	MS-SS	22	MA1-CC2	0.027
Sub. Sed. (SS)	5200	0.05	207	0.7136	MS-SSA	43	MA1-CC3	0.400
Altered MORB (AM)	390	0.05	120	0.7031	MS-GL	61	MA2-CC1	0.003
Sub. Sed. alt. (SSA)	5200	0.05	400	0.7200			MA2-CC2	0.031
Potential magma 1 (MA1)	20	8.00	256	0.7038			MA2-CC3	0.469
Potential magma 2 (MA2)	20	8.00	256	0.7060				
Continent Crust-1 (CC1)	10000	0.05	400	0.7180				
Continent Crust-2 (CC2)	1000	0.05	400	0.7180				
Continent Crust-3 (CC3)	100	0.05	600	0.7180				

a: The end components are defined as follows. MORB source: undergoing 10% of partial melting of upper mantle; GLOSS: global subducting sediments; Sub. Sed.: subducted sediments; Altered MORB: subducted altered oceanic crust; Sub. Sed. alt.: an alternative composition for subducted sediment with more extreme compositions; Potential magma 1: potential composition of magmas with Sr addition of 10% sediments and without He addition; Potential magma 2: potential composition of magmas with Sr addition of 30% sediments and without He addition; Continent crust-1, -2, -3: several potential compositions of crustal components. Most data are from Van Soest et al. (2002); except for the Sr concentrations and isotopic ratios of SS, potential magmas and the $^{87}Sr/^{86}Sr$ ratios of continent crust are from Chu (2005).

b: Mixing curves calculated for the binary mixing of subducted components with the MORB source.

c: $k = ([^4He]/[Sr])_M/([^4He]/[Sr])_{cont}$, where M represents the mixing components starting with an M, and cont represents the other mixing components.

d: Mixing curves calculated for the mixing of the magma as it enters the crust with potential crustal components.

continental crust might be thicker and could cause significant crustal contamination for both Sr-Nd and He systematics. Due to the westward propagating extension of the Okinawa Trough, the thickness of crust underneath KST could become thinner and the mantle gas can degas quickly toward surface without significant crust contamination.

This argument can be against easily by calculating the difference of crustal thickness between present and 10 kyrs ago. Assuming the subsiding rate of the crust is keeping the same rate of 20 mm/y (Liu, 1995) in last 10 kyrs, the total amount of subsidence in this area is only 200 m. It will not make any significant changes for the crustal thickness.

Usually the phenocrysts (e.g., olivine and pyroxene) in the lavas can retain the primary helium isotopic compositions of the magma and can be used for magma genesis discussion. Unfortunately, enough phenogrysts are not available due to the aphyric characteristics of KST lavas, although some olivine and pyroxene crystals can be observed under microscope. Nevertheless, recent study showed that the fluid samples usually exhibit similar helium isotopic compositions of phenocrysts in one area (Van Soest *et al*., 2002). Thus we can assume that the present KST gas samples share the same magma source for the KST lavas. Then, we need to explain the strong continental signatures of low Nd and high Sr isotopic composition for KST lavas, however, high He isotopic composition without crustal signatures for KST gas samples. Van Soest *et al*. (2002) used the plot of ^{3}He/^{4}He vs. ^{87}Sr/^{86}Sr to solve the processes between crustal contamination and subducted sediments contamination. Figure 6A shows the binary mixing model with different end members (parameters shown in Table 4) for the He-Sr isotopic systematics. Assuming that the gas samples sharing the same magma source for the lavas, then we can plot KST and TVG composition into the diagram. It is clear that KST samples fall in the mixing lines of subducted sediments mixing with the MORB source, either with or without helium subduction. It is worthy to note that helium is generally believed to be released at very shallow depth during subducting process and will be not carried into the mantle source (e.g., Staudacher and Allegre, 1988; Hiyagon, 1994). Nevertheless, TVG samples are off the subducted sediments mixing line and fall in the trend of crustal contamination.

Figure 6B further plot the mixing lines for potential magmas with various continent crust components (Table 4). Note that the potential magma 1 (marked as MA1 in Fig. 6B) is the mantle source mixed with 10% Sr composition of subducted sediments without adding helium; similarly, the potential magma 2 (marked as MA2 in Fig. 6B) is mixed with 30% of subducted sediments. Then, the potential magmas mix with different continental crust end members in crustal level. The TVG samples fall in the range of MA1 mixing with 2–5% continental crusts; nevertheless, KST samples exhibit similar compositions of MA2 and do not need any crust input. This result is supported by the recent work of Chu (2005) that the KST magma results from the partial melting of subducted sediments and altered oceanic crust and then reacted with mantle component.

Concluding Remarks

(1) Similar with TVG gas samples, the KST gas samples exhibit typical compositions of low temperature fumaroles in the world, i.e., with high CO_2 and H_2S but low SO_2 and HCl contents.

(2) KST gas samples fall in the range of compositions of divergent plate and hot spot gases; however, TVG gases belong to the compositions of convergent plate gases. It implies that they may be derived from different tectonic environments.

(3) KST gas samples exhibit consistent high helium isotopic compositions, ranging from 7.4 to 8.4 R_A after air correction. It indicates that mantle component play an important role for the gas source in the area. The high helium isotopic data around KST can further suggest that there is a magma reservoir underneath KST and can induce current active hydrothermal activity both on-land and submarine in the region.

(4) Samples from I-Lan Plain also show elevated $^3He/^4He$ ratios, estimated proportion of mantle components range from <1% to 19%. It implies that the mantle fluids may have invaded into I-Lan Plain via a blind fault or magma intrusion in southern part of I-Lan Plain.

(5) He-Sr binary mixing model demonstrates that KST samples experienced minimum crustal contamination; whereas, TVG samples need 2–5% continental crusts input the magma to explain their helium-strontium isotopic data.

Acknowledgments—We thank Messrs. N. T. Liu, H. H. Ho, K. W. Wu, W. L. Hong, D. R. Hsiao, B. W. Lin and C. C. Wang at the Department of Geosciences of NTU for help with collecting and analyzing samples. Drs. Y. Sano, S. L. Chung, China Chen, S. R. Song, K. L. Wang, C. H. Lin and S. Tsao gave valuable suggestions during different stages of this work. Two anonymous referees reviewed the manuscripts and gave critical comments and suggestions to improve the manuscript. The National Science Council (TFY/89-2116-M-002-040; 90-2116-M-002-009; 91-2116-M-002-017) and Central Geological Survey of Taiwan financially supported this research.

References

Chen, C-H. (1990) *Igneous Rocks in Taiwan*. Cent. Geol. Surv., MOEA, Taiwan, ROC, 137 pp. (in Chinese).

Chen, C. H. and Shen, J. J. S. (2005) A refined historical record of volcanic eruptions around Taiwan: tectonic implications in the arc-continent collision area. *Terr. Atmos. Oceanic Sci.* **16**, 331–343.

Chen, C. H., Lee, T., Shieh, Y. N., Chen, C-H. and Hsu, W. Y. (1995) Magmatism at the onset of back-arc basin spreading in the Okinawa Trough. *Jour. Volcanol. Geotherm. Res.* **69**, 313–322.

Chen, C. T. A., Wang, B. J., Huang, J. F., Lou, J. Y., Kuo, F. W., Tu, Y. Y. and Tsai, H. S. (2005a) Investigation into extremely acidic hydrothermal fluids off Kueishantao islet, Taiwan. *Acta Ocean. Sinica* **24**, 125–133.

Chen, C. T. A., Zeng, Z., Kuo, F. W., Yang, T. F., Wang, B. J. and Tu, Y. Y. (2005b) Tide-influenced acidic hydrothermal system offshore NE Taiwan. *Chem. Geol.* doi:10.1016/j.chemgeo.2005.07.022 (in press).

Chen, Y. G., Wu, W. S., Chen, C-H. and Liu, T. K. (2001) A date for volcanic-eruption inferred from a siltstone xenolith. *Quat. Sci. Rev.* **20**, 869–873.

Chiodini, G., Frondini, F., Cardellini, C., Granieri, D., Marini, L. and Ventura, G. (2001) CO_2 degassing and energy release at Solfatara volcano, Campi Flegrei, Italy. *J. Geophys. Res.* **106**, 16213–16221.

Chu, C. H. (2005) Generation of high-Mg andesites in the Kueishantao volcano, the southernmost part of the Okinawa Trough. MS thesis, Inst. Geosciences, National Taiwan Univ., 99 pp. (in Chinese with English abstract).

Chung, S. L., Wang, S. L., Shinjo, R., Lee, C. S. and Chen, C. H. (2000) Initiation of arc magmatism in an embryonic continental rifting zone of the southernmost part of Okinawa Trough. *Terra Nova* **12**, 225–230.

Delmelle, P. and Stix, J. (2000) Volcanic gases. *Encyclopedia of Volcanoes* (Sigurdsson, H. *et al*., eds.), 803–815, Academic Press.

Farley, K. A. and Neroda, E. (1998) Noble gases in the Earth's mantle. *Ann. Rev. Earth Planet. Sci.* **26**, 189–218.

Fu, C. C., Yang, T. F., Walia, V. and Chen, C-H. (2005) Reconnaissance of soil gas composition over the buried fault and fracture zone in southern Taiwan. *Geochem. J.* **39**, this issue, 427–439.

Giggenbach, W. F. (1975) A simple method for the collection and analysis of volcanic gas samples. *Bull. Volcanol.* **36**, 132–145.

Giggenbach, W. F. and Matsuo, S. (1991) Evaluation of results from second and third IAVCEI field workshop on volcanic gases, Mt. Usu, Japan and White Island, New Zealand. *Appl. Geochem.* **6**, 125–141.

Giggenbach, W. F., Tedesco, D., Sulistiyo, Y., Caprai, A., Cioni, R., Favara, R., Fischer, T. P., Hirabayashi, J.-I., Korzhinsky, M., Martini, M., Menyailov, I. and Shinohara, H. (2001) Evaluation of results from the fourth and fifth IAVCEI field workshops on volcanic gases, Vulcano island, Italy and Java, Indonesia. *Jour. Volcanol. Geotherm. Res.* **108**, 157–172.

Hilton, D. R., Barling, J. and Wheller, G. E. (1995) Effect of shallow-level contamination on the helium isotope systematics of ocean-island lavas. *Nature* **373**, 330–333.

Hilton, D. R., Fischer, T. P. and Marty, B. (2002) Noble gases and volatile recycling at subduction zones. *Noble Gases in Geochemistry and Cosmochemistry* (Porcelli, D. *et al*., eds.), *Reviews in Mineralogy and Geochemistry* **47**, 319–370.

Hiyagon, H. (1994) Retention of helium in subducted interplanetary dust particles. *Science* **265**, 1257–1259.

Hsu, L. C. (1963) Petrology of the Pleistocene andesite from Kueishantao, Northern Taiwan. *Acta Geol. Taiwan.* **10**, 29–40.

Hsu, S. K. (2001) Lithospheric structure, buoyancy and coupling across the southernmost Ryukyu subduction zone: an example of decreasing plate coupling. *Earth Planet. Sci. Lett.* **186**, 471–478.

Hsu, S. K., Sibuet, J.-C., Monti, S., Shyu, C. T. and Liu, C. S. (1996) Transition between the Okinawa Trough backarc extension and the Taiwan collision: New insights on the

southernmost Ryukyu subduction zone. *Mar. Geophys. Res.* **18**, 163–241.

Kao, H. Shen, S. J. and Ma, K. F. (1998) Transition from oblique subduction to collision: earthquakes in the southernmost Ryukyu arc-Taiwan region. *J. Geophys. Res.* **103**, 7211–7229.

Lee, C. S., Shor, G., Jr., Bibee, L. D., Lu, R. S. and Hilde, T. W. C. (1980) Okinawa Trough: Origin of a back-arc basin. *Mar. Geol.* **35**, 219–241.

Lee, C. S., Tsai, C. F., Chung, S. L. and SPOT members (1998) Active interaction of submarine volcanoes and ocean current in the southernmost Okinawa Trough. *Eos Trans. AGU*, **79**(45), Fall Meet Suppl., F858.

Lee, H. F., Yang, T. F., Lan, T. F., Song, S. R. and Tsao, S. (2005) Fumarolic gas compositions of Tatun Volcano Group, northern Taiwan. *Terr. Atmos. Oceanic Sci.* **16**, 843–864.

Letouzey, J. and Kimura, M. (1986) The Okinawa Trough: Genesis of a back-arc basin developing along a continental margin. *Tectonophys.* **125**, 209–230.

Lin, C. H., Konstantinou, K. I., Liang, W. T., Pu, H. C., Lin, Y. M., You, S. H. and Huang, Y. P. (2005) Preliminary analysis of volcanoseismic signals recorded at the Tatun Volcano Group, northern Taiwan. *Geophys. Res. Lett.* **32**, L10313, doi:10.1029/2005GL022861.

Lin, J. Y., Hsu, S. K. and Sibuet, J.-C. (2004) Melting features along the western Ryukyu slab edge (northeast Taiwan): Tomographic evidence. *J. Geophys. Res.* **109**, B12402, doi:10.1029/2004JB003260.

Liu, C. C. (1995) The Ilan plan and the southwestward extending Okinawa Trough. *Jour. Geol. Soc. China* **38**, 229–242.

Lupton, J. E. (1983) Terrestrial inert gases: isotopes tracer studies and clues to primordial components in the mantle. *Ann. Rev. Earth Planet. Sci.* **11**, 371–414.

Macpherson, C. G., Hilton, D. R., Sinton, J. M., Poreda, R. J. and Craig, H. (1998) High $^3He/^4He$ ratios in the Manus backarc basin: Implications for mantle mixing and the origin of plumes in the western Pacific Ocean. *Geology* **26**, 1007–1010.

Matsuda, J., Matsumoto, T., Sumino, H., Nagao, K., Yamamoto, J., Miura, Y., Kaneoka, I., Takahata, N. and Sano, Y. (2002) The $^3He/^4He$ ratio of the new internal He standard of Japan (HESJ). *Geochem. J.* **36**, 191–195.

Notsu, K., Nakai, S., Igarashi, G., Ishibashi, J., Mori, T., Suzuki, M. and Wakita, H. (2001) Spatial distribution and temporal variation of $^3He/^4He$ in hot spring gas released from Unzen volcanic area, Japan. *Jour. Volcanol. Geotherm. Res.* **111**, 89–98.

Ozima, M. and Podosek, F. A. (2002) *Noble Gas Geochemistry*. 2nd ed., Cambridge University Press, Cambridge, 286 pp.

Park, J.-O., Tokuyama, H., Shinohara, M., Suyehiro, K. and Taira, A. (1998) Seismic record of tectonic evolution and backarc rifting in the southern Ryukyu island arc system. *Tectonophys.* **294**, 21–42.

Porcelli, D., Ballentine, C. J. and Wieler, R. (2002) An overview of noble gas-geochemistry and cosmochemistry. *Noble Gases in Geochemistry and Cosmochemistry* (Porcelli, D. *et al.*, eds.), *Reviews in Mineralogy and Geochemistry* **47**, 1–19.

Poreda, R. and Craig, H. (1989) Helium isotope ratios in circum-Pacific volcanic arcs. *Nature* **338**, 473–478.

Poreda, R. J., Jeffery, A. W. A., Kaplan, I. R. and Craig, H. (1988) Magmatic helium in subduction-zone natural gases. *Chem. Geol.* **71**, 199–210.

Sano, Y. and Wakita, H. (1985) Geographical distribution of $^3He/^4He$ ratios in Japan: implications for arc tectonics and incipient magmatism. *J. Geophys. Res.* **90**, 8729–8741.

Sano, Y., Nakamura, Y. and Wakita, H. (1984) Helium-3 emission related to volcanic activity. *Science* **224**, 150–151.

Shaw, A. M, Hilton, D. R., Macpherson, C. G. and Sinton, J. M. (2004) The CO_2-He-Ar-H_2O systematics of the Manus back-arc basin: Resolving source composition from degassing and contamination effects. *Geochim. Cosmochim. Acta* **68**, 1837–1856.

Sibuet, J.-C., Deffontaines, B., Hsu, S. K., Thareau, N., Le Formal, J.-P., Liu, C. S. and the ACT party (1998) The Okinawa Trough backarc basin: early tectonic and magmatic evolution. *J. Geophys. Res.* **103**, 30245–30267.

Song, S. R., Yang, T. F., Yeh, Y. H., Tsao, S. and Lo, H. J. (2000) The Tatun Volcano Group is active or extinct? *Jour. Geol. Soc. China* **43**, 521–534.

Staudacher, T. and Allegre, C. (1988) Recycling of oceanic crust and sediments: the noble gas subduction barrier. *Earth Planet. Sci. Lett.* **89**, 173–183.

Teng, L. S. (1996) Extensional collapse of the northern Taiwan mountain belt. *Geology* **24**, 949–952.

Tsai, Y. B., Feng, C. C., Chiu, J. M. and Liao, H. B. (1975) Correlation between microearthquakes and geologic faults in the Hsintien-Ilan area. *Petrol. Geol. Taiwan* **12**, 149–167.

Van Soest, M. C., Hilton, D. R. and Kreulen, R. (1998) Tracing crustal and slab contributions to arc magmatism in the Lesser Antilles island arc using helium and carbon relationships in geothermal fluids. *Geochim. Cosmochim. Acta* **62**, 3323–3335.

Van Soest, M. C., Hilton, D. R., Macpherson, C. G. and Mattey, D. P. (2002) Resolving sediment subduction and crustal contamination in the Lesser Antilles island arc: A combined He-O-Sr isotope approach. *J. Petrol.* **43**, 143–170.

Wang, K. L., Chung, S. L., Chen, C. H., Shinjo, R., Yang, T. F. and Chen, C-H. (1999) Post-collisional magmatism around northern Taiwan and its relation with opening of the Okinawa Trough. *Tectonophys.* **308**, 363–376.

Wang, K. L., Chung, S. L., O'Reilly, S. Y., Sun, S.-s., Shinjo, R. and Chen, C. H. (2004) Geochemical constraints for the genesis of post-collisional magmatism and the geodynamic evolution of the northern Taiwan region. *J. Petrol.* **45**, 975–1011.

Yang, T. F. (2000) The helium isotopic ratios of fumaroles from Tatun Volcano Group of Yangmingshan National Park, N. Taiwan. *Journal of National Park* **10**, 73–94. (in Chinese with English abstract).

Yang, T. F., Chen, C-H., Tien, R. L., Song, S. R. and Liu, T. K. (2003a) Remnant magmatic activity in the Coastal Rang of East Taiwan after arc-continent collision: fission-track date and $^3He/^4He$ ratio evidence. *Radiat. Meas.* **36**, 343–349.

Yang, T. F., Chou, C. Y., Chen, C-H., Chyi, L. L. and Jiang, J. H. (2003b) Exhalation of radon and its carrier gases in SW Taiwan. *Radiat. Meas.* **36**, 425–429.

Yang, T. F., Sano, Y. and Song, S. R. (1999) $^3He/^4He$ ratios of fumaroles and bubbling gases of hot springs in Tatun Volcano Group, North Taiwan. *Il Nuovo Cimento* **22C**, 281–286.